Radiotherapy and Oncology 136 (2019) 71–77

Contents lists available at ScienceDirect

Radiotherapy and Oncology

journal homepage: www.thegreenjournal.com

Original Article

Composite minimax robust optimization of VMAT improves target coverage and reduces non-target dose in head and neck cancer patients

Dirk Wagenaar [a,*,1], Roel G.J. Kierkels [a,1], Jeffrey Free [a], Johannes A. Langendijk [a], Stefan Both [a], Erik W. Korevaar [a]

[a] Department of Radiation Oncology, University Medical Center Groningen, University of Groningen, the Netherlands

ARTICLE INFO

Article history:
Received 14 November 2018
Received in revised form 15 February 2019
Accepted 20 March 2019
Available online 11 April 2019

Keywords:
Robust optimization
Head-and-neck cancer
Normal tissue complication probability
Adaptive radiotherapy
Dose accumulation
Volumetric modulated arc therapy

ABSTRACT

Background and purpose: To assess the potential of composite minimax robust optimization (CMRO) compared to planning target volume (PTV)-based optimization for head and neck cancer (HNC) patients treated with volumetric modulated arc therapy (VMAT).

Materials and methods: Ten HNC patients previously treated with a PTV-based VMAT plan were studied. In addition to the PTV-plan a VMAT plan was created with CMRO. For both plans an adapted planning strategy was also investigated, including a plan adaptation during the third week of treatment. The PTV-plans and CMRO-plans (adapted and non-adapted) were evaluated by means of the estimated actually given dose (EAGD). Therefore, the dose was calculated on daily acquired CBCTs, mapped onto the planning CT and accumulated. The plans were compared by dosimetric parameters and normal tissue complication probabilities (NTCPs) for tube feeding dependence, grade 2–4 dysphagia and xerostomia. The accuracy of CBCT-based dose accumulation was further quantified by comparisons of dose accumulation on weekly verification CTs.

Results: On average, CMRO significantly increased (1.5 Gy) the $D_{98\%}$ of the EAGD to the clinical target volume and significantly decreased the mean dose of the ipsilateral parotid (2.8 Gy), inferior pharynx constrictor muscle (0.7 Gy) and the oral cavity (0.8 Gy). This translated into significantly reduced NTCP of tube feeding dependence (0.9%) and xerostomia (2.8%). The differences in EAGD derived from evaluation CTs or CBCTs were minimal.

Conclusion: Minimax robust optimization led to improved target coverage and dose reduction in organs at risk in HNC patients treated with VMAT.

 Radiotherapy and Oncology 136 (2019) 71–77

The primary goal of radiotherapy is to adequately treat the clinical target volume (CTV) with a uniform dose. The CTV is however subject to geometrical variations and setup uncertainties. The traditional approach to avoid underdosage during the fractionated treatment course is to apply a planning target volume (PTV) margin around the CTV [1–3]. This approach should lead to adequate PTV coverage on the planned dose distribution and adequate coverage of the CTV during the treatment course.

The use of a PTV margin is based on the assumption that the dose distribution is invariant. However, setup errors and geometrical variations affect the shape of the dose distribution, especially in the vicinity of density gradients. PTV-less optimization approaches have been described in literature that provide a superior balance between tumor control rate and normal tissue toxicity. These optimization approaches are referred to as robust optimization [4–10].

Two approaches to robust planning optimization have been introduced: probabilistic planning and minimax optimization [11,12]. The probabilistic approach consists of optimizing the expectation value of objectives based on an *a priori* probability density function of geometric errors. Recently, Witte et al. investigated the potential clinical benefit of PTV-less probabilistic planning in a spherical phantom [10]. They demonstrated that an indentation of the 95% dose level by one third of the margin size at a strictly uniform dose distribution at prescription level is feasible without sacrificing tumor dose confidence. Fontanaroza et al. demonstrated probabilistic planning for IMRT in head and neck cancer (HNC) patients and found improved organ-at-risk (OAR) sparing as compared to PTV-based plans, with comparable CTV coverage [5]. The minimax robust optimization approach instead optimizes the objective value in the worst-case based on a positioning inaccuracy in different directions. In contrast to the probabilistic approaches in which a probability distribution is needed, the minimax robust optimization approach only requires information about the scenarios to include. Fredriksson et al. proposed an

* Corresponding author at: P.O. Box 30.001, 9700 RB Groningen, the Netherlands.
E-mail address: ir.d.wagenaar@gmail.com (D. Wagenaar).
[1] These authors contributed equally to the research described in this manuscript.

https://doi.org/10.1016/j.radonc.2019.03.019
0167-8140/

implementation of minimax robust optimization which aims to optimize the objective function of the physically realistic composite worst-case scenario [13]. In a recent study, this composite minimax robust optimization (CMRO) was found to give a sharper dose fall-off than other implementations [14].

CMRO was previously evaluated in static and dynamic phantoms [15,16]. Both studies demonstrated improved target uniformity compared to PTV-based planning methods, especially near heterogeneous density regions. Since these phantom studies have demonstrated great potential also for OAR sparing, we evaluated the CMRO in detail for adaptive photon therapy in HNC patients.

The aim of this study was to assess the benefit of CMRO compared to PTV-based optimization in HNC patients treated with VMAT in terms of CTV coverage and dose to non-target tissues.

Materials and methods

Patients and treatment

The study population consisted of ten patients with stage II-IV squamous cell HNC with various tumor locations: paranasal sinus (2); nasopharynx (3); glottic larynx (1); hypopharynx (1); oropharynx (3). The tumor stages varied between T1-4N0-2M0. All patients reported their xerostomia as 'None' or 'a bit' according to the EORTC QLQ-H&N35 and their weight loss prior to treatment was none (5) or 1–10% (5). None of the patients had a percutaneous endoscopic gastrostomy tube before start of treatment.

All patients were previously treated with a simultaneous integrated boost technique consisting of a prescription of 70.00 Gy to the therapeutic CTV and 54.25 Gy to the prophylactic CTV in 35 fractions using VMAT [15]. The PTVs were created using a 5.0 mm uniform expansion of their respective CTVs. Plans were optimized aiming at V95% $\geq$98% of the PTV while limiting the maximum spinal cord dose to 54.00 Gy and the maximum brain dose to 60.00 Gy. The mean dose to the parotid glands and swallowing muscles were reduced as much as possible. All clinical plans were created by a dosimetrist specialized in HNC planning. Patients were immobilized using an individualized neck cushion and a 5-points mask. Online patient positioning verification was performed daily using CBCT imaging. In addition, verification CTs were acquired on a weekly basis outside the treatment room. In total 350 CBCTs and 70 verification CTs were analyzed.

Treatment plan optimization

Planning was performed in the RayStation (RaySearch Laboratories AB, Stockholm, Sweden) treatment planning system (TPS). Clinical PTV-plans were created in version 5.0 and its adjustments in version 4.99, which is the research build of the same version. The clinical PTV-plan was further optimized to create a reference 'PTV-plan'. In addition, a copy of the clinical PTV-plan was used to create the CMRO-plan in which only the target objectives were changed into their respective CTVs. Next, the CMRO-plan was optimized using the CMRO algorithm [13]. The CMRO algorithm minimized the cost function of the worst out of seven scenarios which consisted of the nominal scenario and 5.0 mm shifts of the isocenter in the planning CT in the lateral, longitudinal and transverse directions. Each plan was optimized with the same objective weights for 200 iterations or when an optimal solution (tolerance <1e−5) was reached. All plans had an isotropic dose grid resolution of 3.0 mm.

To ensure equal target coverage, the CMRO-plan and PTV-plan were normalized such that the $D_{98\%}$ of the CTVs received at least 95% of the prescribed dose in the voxel-wise minimum dose. Since CMRO is referred to as margin-less planning, the PTV could not be used for plan normalization. Moreover, Harrington et al. illustrated that the voxel-wise minimum dose can be interpreted similarly to the PTV dose of the nominal plan [16]. The voxel-wise minimum dose was derived from 14 perturbed scenarios by rigidly shifting the isocenter in the planning CT with 5.0 mm in the lateral, longitudinal and transverse directions and their diagonals. The voxel-wise minimum dose distribution was then derived as a composite of the minimum dose voxels of all scenarios. This approach is described in more detail in a previous study [17].

CBCT dose calculation, mapping and accumulation

The workflow for simulating the treatment course to calculate the EAGD is shown in Fig. 1. Deformable image registration was performed between each CBCT and planning CT with the algorithm implemented in the TPS and previously described by Weistrand et al. [18]. In most cases, the field-of-view (FOV) of the CBCTs did not capture the shoulders and cranial end of the skull. In these cases, the patient external was mapped from the planning CT to the CBCT. Next, the density of the volume inside the external, but outside the CBCT's FOV was assigned a density of 1.00 g cm^{-3}. The dose of the PTV- and CMRO-plans was recalculated on a segmented CBCT. Segmentation was based on the TPS' default settings. In the last step, the dose distributions of all CBCTs were mapped to the planning CT and summed to get the EAGD.

Plan adaptations

To investigate CMRO in an adaptive setting, we adapted both the PTV-plan and CMRO-plan after three weeks of treatment if the sum of the three normal tissue complication probabilities (NTCP) under investigation (see subsection below) increased by +2.5% for the PTV-plan or that the CTVs were underdosed (i.e. $D_{98\%}$ <95%) for the PTV-plan. Plans were adapted by re-optimizing the dose on the verification CT using the PTV-based optimization for the PTV-plan and CMRO for the CMRO-plan. Hence, the plan quality was assessed from the EAGD in terms of target coverage, OAR dose and NTCPs. The EAGD of the adapted treatment schedule was derived from the dose of the first 15 fractions using the nominal plan and the remaining fractions using the dose of the adapted plan.

CBCT-based dose accumulation validation

Dose re-calculations on the verification CTs were used to validate the accuracy of the EAGD derived from CBCTs. This, together with dose re-calculations on two different sets of weekly CBCTs were used to estimate the difference in EAGD due to the use of CBCTs instead of verification CTs.

Analysis

The CMRO-plans were compared against the PTV-plans using dosimetric parameters of the EAGD of the CTVs and OARs. The investigated OARs reflected those used in our clinical practice. Target coverage conformity was defined by the conformity index (CI) [19]:

$$\mathrm{CI} = 2\frac{V_{\mathrm{intersect}}}{V_{\mathrm{CTV}} + V_{95\%}}$$

where $V_{\mathrm{intersect}}$ is the absolute volume of the CTV that received 95% of the prescribed dose and V_{CTV} is the volume of the CTV. Target homogeneity was defined as:

$$\mathrm{HI} = \frac{D_{2\%} - D_{98\%}}{D_p}$$

where D_{p} is the prescribed dose to the target [3]. To derive the HI of the prophylactic CTV the primary CTV (+5.0 mm) was excluded

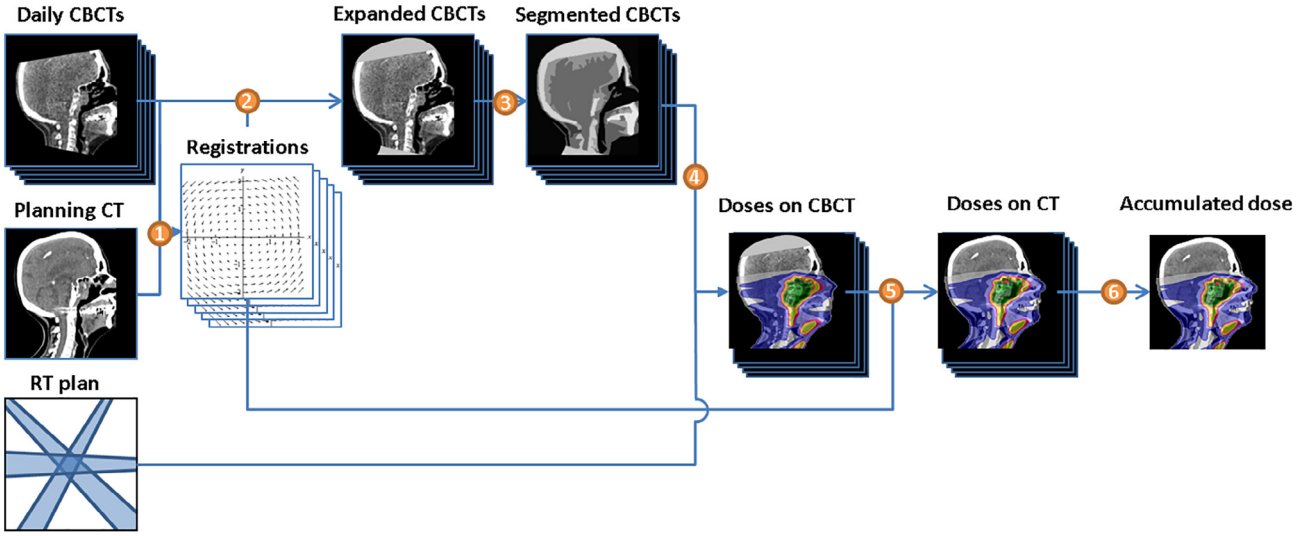

Fig. 1. Schematic representation of the workflow to calculate the estimated actually given dose. 1: A deformable image registration is made for all 35 individual CBCTs to the planning CT. 2: The external of the planning CT is warped towards each CBCTs, the part of the external that is outside the CBCT's field of view is overridden with a density of water. 3: The CBCTs are automatically segmented based on their CT value into air, lung, adipose, soft tissue, cartilage/bone and other (i.e. higher densities) to allow dose calculation. 4: The dose of the treatment plan is calculated on the segmented CBCTs resulting in a daily dose distribution. When a treatment plan-adaptation is considered, the first 15 fractions are calculated using the original treatment plan and the remaining 20 fractions using the adapted treatment plan. 5: All doses are deformed to the planning CT using the registrations created in step 1. 6: The individual doses are summed resulting in the estimated actually given dose distribution.

from it. In addition, all plans were evaluated by NTCP values for xerostomia [20], grade 2–4 dysphagia [20], and tube feeding dependence [21].

A paired Wilcoxon signed-rank test was used to calculate two-tailed p-values (R-Project 3.5.1, Vienna, Austria). The statistical significance was determined after accounting for multiple testing using Bonferroni's correction [22]. Differences were considered statistically significant if $p < 0.005$ ($\alpha = 0.05/10$ structures) for OAR doses, $p < 0.008$ ($\alpha = 0.05/6$ parameters) for target coverage and $p < 0.017$ ($\alpha = 0.05/3$ NTCPs) for NTCPs.

Results

The difference in EAGD between a PTV-plan and a CMRO-plan without plan adaptation for a typical case is shown in Fig. 2. This case illustrates a higher dose to the target areas and a dose reduction to the organs at risk, particularly in the areas with high density gradients such as near bone and the esophagus. Similar dose differences were observed in the other cases.

Robust optimization without plan adaptation

The average EAGD for both the PTV-plan and CMRO-plan without plan adaptation are shown in Table 1 and Fig. 3. The $D_{98\%}$ of the EAGD was significantly higher in the CMRO-plans compared to the reference PTV-plans for the prophylactic CTV ($\Delta D_{98\%} = 1.5$ Gy; 95% CI = 1.0–2.0 Gy; $p = 0.002$) and significantly lower dose to the ipsilateral parotid gland ($\Delta D_{mean} = 2.8$ Gy; 95%CI = 1.6–4.0 Gy; $p = 0.004$), the inferior PCM ($\Delta D_{mean} = 2.7$ Gy; 95%CI = 0.4–5.0 Gy; $p = 0.002$) and the oral cavity ($\Delta D_{mean} = 0.7$ Gy; 95%CI = 0.4–1.0 Gy; $p = 0.004$). The CMRO-plans also led to lower NTCP values for tube feeding dependence (ΔNTCP = 0.9%; 95%CI = 0.4–1.4%; $p = 0.004$) and xerostomia (ΔNTCP = 2.8%; 95%CI = 1.5–4.1%; $p = 0.006$) compared the PTV-plans (Table 1 and Fig. 4).

The nominal dose distribution of the CMRO-plan showed significantly higher dose to the primary and prophylactic CTVs and significantly lower dose to the ipsilateral parotid gland, the inferior and superior PCM and the oral cavity compared to the PTV-plans. The NTCP values derived from the nominal dose were within 0.5% of the values calculated from the EAGD for both the CMRO-plan and PTV-plan.

Robust optimization with plan adaptation

CTV underdosage was not observed in the studied patients. However, the ΣNTCP of 4/10 patients exceeded the 2.5% threshold after three weeks of treatment. Table 2 shows the results based on the EAGD derived from the adapted and non-adapted PTV-based and CMRO-based treatment simulations. In these four patients, the mean dose in the OARs was on average 1.1 (range: −1.1 to 3.1) Gy lower in the CMRO-plans than the PTV-based approach (Table 2). The plan adaptation resulted into an additional 0.7 (range: −0.5 to 1.2) Gy dose reduction to the OARs. For these patients, the estimated NTCPs were on average reduced by 5.8% and 7.9% using an adapted PTV-plan and adapted CMRO plan, respectively.

CBCT-based dose accumulation validation

The absolute difference of the $D_{98\%}$ of both CTVs derived from a set of weekly CBCTs and verification CTs was on average 0.5 Gy and the differences in NTCP values was on average 0.6% (Supplement Fig. S.1). Comparing the dose from two different sets of weekly CBCTs, this difference was 0.1 Gy for the CTVs and 0.3% for the NTCP values.

Discussion

We evaluated CMRO in VMAT of head and neck cancer patients, and assessed plan robustness using the estimated actual given dose. It was demonstrated that CMRO resulted in approximately 2 Gy lower mean dose to several OARs with similar or improved CTV coverage as compared to conventional PTV-based plans. On average, CMRO led to around a 2.3 Gy average dose decrease in the parotids, pharyngeal muscle superior, cricopharyngeal muscle and the supraglottic larynx and a 1.7 Gy increase of the $D_{98\%}$ of the primary and elective CTVs.

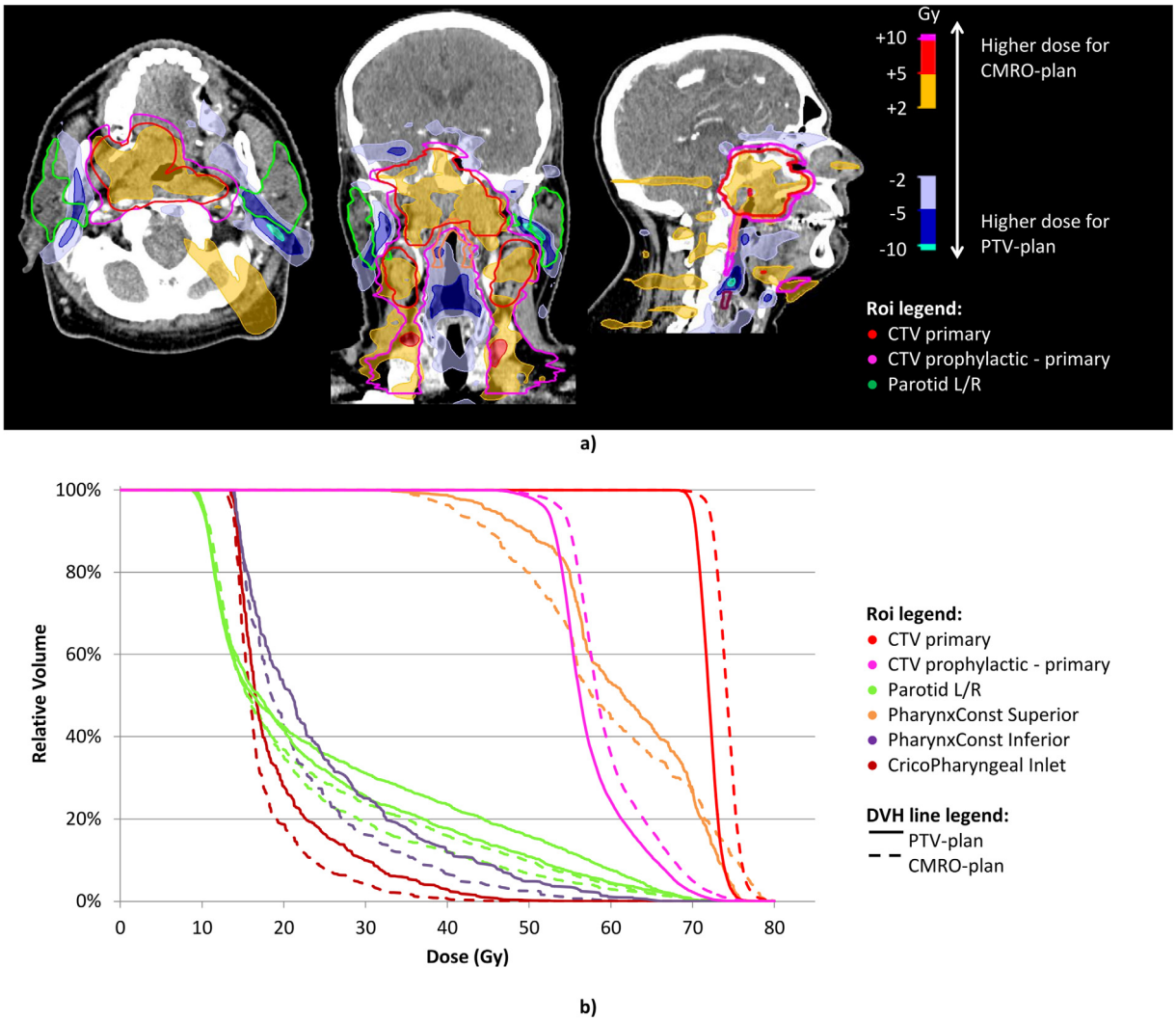

Fig. 2. Differences in estimated actually given dose for a PTV optimized and a robustly optimized VMAT treatment plan: typical case (a) Difference in estimated actually given dose distribution. (b) Dose–volume histogram of the estimated actually given dose for both treatment plans.

Other studies, albeit on different treatment sites, show similar results with CMRO in terms of OAR dose sparing. It was shown for CMRO in breast cancer patients that target coverage improved at identical or reduced OAR dose [6,23]. The agreement between the planned nominal dose and dose evaluated on the 4DCT was better for the CMRO-plans than the PTV-plans [6]. Archibald-Heeren et al. compared CMRO VMAT of lung cancer on a thorax phantom [24]. The authors found fewer maximum and minimum dose variations compared to other current treatment techniques such as internal target volume based planning as evaluated on a 4DCT [24]. Zhang et al. investigated the benefit of CMRO for five prostate cancer patients in which the CTV and OAR delineations were shifted inside the patient to create different scenarios [25]. Their method did not include a dose recalculation per scenario and accounted for internal target motion rather than patient positioning errors. They reported a mean dose reduction of 6.4% and 19.7% for the rectal and bladder walls, respectively. Previous studies on CMRO of proton therapy found larger benefits for CMRO, which was expected due to the inherent lack of dose invariance of the treatment modality [4,13,26].

In terms of toxicity probabilities, the various NTCPs decreased approximately 1–3% for the CMRO plans as compared to the PTV-plans. The NTCP models were derived from planned dose distributions, whereas the NTCPs in this study were derived from the EAGD. Since the EAGD is potentially more directly related to toxicity than the planned nominal dose, this could lead to a slight underestimation of the improvement in toxicity probability. However, the NTCP values of the planned dose distribution were very similar to those from the EAGD (Table 1). Therefore, we expect these results to be representative.

We demonstrated that CMRO led to improved robustness compared to PTV-based optimization, at no expense of OAR dose. Other factors affecting the plan robustness are the magnitude of robustness shifts (or PTV margin) and the number of plan adaptations. In this study, we found, albeit on 4/10 patients, that CMRO led to an improved dose distribution when using plan adaptations after three weeks of treatment, indicating that CMRO can be used in combination with adaptive radiotherapy. Furthermore, it can be argued that CMRO may lead to fewer plan adaptations than PTV-based optimization. This was however not investigated.

In this study, the EAGD was derived from dose calculations on daily acquired CBCTs that were mapped to the reference CT and accumulated. We acknowledge that the deformable image registration (required for dose mapping) introduces new unknown errors [27]. The dose calculation was performed using a segmentation of the CBCT based on six tissue substitutes. Based on the

Table 1
The average dosimetric parameters and NTCP values of the PTV-optimized and CMRO treatment plans.

	Nominal dose (N = 10)		EAGD (CBCT, N = 10)		EAGD (CT, N = 10)	
	PTV-plan	CMRO-plan	PTV-plan	CMRO-plan	PTV-plan	CMRO-plan
Dmean of OARs (Gy)						
Ipsi parotid	31.9 (27.3–37.1)	29.1 (25.0–33.9)*	32.7 (28.2–37.6)	29.8 (25.8–34.5)*	34.0 (29.3–39.2)	31.2 (26.8–36.0)*
Contra parotid	23.7 (19.0–29.2)	21.4 (16.8–26.0)	24.0 (19.3–29.4)	21.7 (17.3–26.3)	24.0 (19.3–29.5)	21.7 (17.3–26.3)*
Submand. Right	53.4 (37.8–68.9)	53.3 (37.5–69.1)	53.2 (37.7–68.6)	53.0 (37.3–68.8)	53.5 (37.6–69.4)	53.3 (37.1–69.5)
Submand. Left	57.8 (47.3–68.2)	58.3 (47.4–68.9)	57.9 (47.9–67.8)	58.4 (48.0–68.4)	58.1 (47.4–68.6)	58.6 (47.5–69.3)
Inferior PCM	40.8 (31.0–53.1)	38.1 (28.1–50.9)*	41.4 (31.9–53.4)	38.7 (29.1–51.1)*	40.6 (31.1–52.6)	38.2 (28.6–50.6)*
Superior PCM	51.5 (42.3–63.6)	50.7 (41.3–62.8)*	51.8 (42.6–63.9)	51.1 (41.7–63.2)	52.4 (43.3–64.3)	51.8 (42.5–63.7)
Cricopharyngeus M.	23.2 (16.5–28.8)	21.0 (15.3–26.1)	22.6 (16.8–27.7)	20.8 (15.4–25.7)	23.2 (17.2–28.5)	21.1 (15.9–25.7)*
Supraglottic larynx	33.8 (22.8–43.1)	31.8 (20.6–41.4)	35.5 (24.2–44.5)	33.4 (22.0–42.9)	34.6 (23.4–44.3)	32.8 (21.3–42.8)
Oral cavity	40.5 (33.8–48.2)	39.7 (32.8–47.4)*	40.7 (34.0–48.4)	39.9 (33.1–47.6)*	40.8 (34.1–48.5)	40.1 (33.2–47.7)*
Spinal cord (D2)	43.8 (39.2–48.2)	44.7 (40.1–48.8)	44.2 (40.2–48.0)	45.0 (40.9–48.6)	43.5 (38.9–47.9)	44.4 (39.8–48.4)
Target coverage						
$D_{98\%}$ $CTV_{primary}$ (Gy)	69.2 (68.6–69.8)	71.3 (70.4–72.1)*	69.2 (68.6–69.8)	71.1 (70.1–72.0)	69.6 (69.0–70.2)	71.3 (70.3–72.2)
$D_{98\%}$ $CTV_{prophylactic}$ (Gy)	55.3 (52.6–57.6)	57.1 (54.4–59.4)*	55.0 (52.2–57.4)	56.5 (54.1–58.8)*	55.5 (52.8–57.8)	56.9 (54.4–59.0)*
CI $CTV_{primary}$	0.52 (0.46–0.58)	0.53 (0.47–0.59)	0.52 (0.46–0.58)	0.53 (0.47–0.60)	0.52 (0.46–0.58)	0.53 (0.47–0.59)
CI $CTV_{prophylactic}$	0.51 (0.46–0.55)	0.51 (0.46–0.55)	0.50 (0.44–0.55)	0.50 (0.43–0.56)	0.51 (0.47–0.55)	0.51 (0.47–0.56)
HI $CTV_{primary}$	0.92 (0.91–0.93)	0.92 (0.91–0.94)	0.92 (0.92–0.94)	0.92 (0.91–0.93)	0.93 (0.92–0.94)	0.92 (0.91–0.93)
HI $CTV_{prophylactic}$	0.74 (0.69–0.78)	0.75 (0.71–0.78)	0.72 (0.67–0.76)	0.72 (0.68–0.77)	0.72 (0.68–0.75)	0.72 (0.68–0.76)
NTCPs (%)						
Tube feeding dep.	8.7 (4.6–11.7)	7.7 (4.0–10.4)*	8.9 (4.5–12.1)	8.0 (4.0–10.9)*	9.1 (4.6–12.4)	8.2 (4.1–11.2)*
Grade 2–4 dysphagia	27.1 (21.3–34.1)	26.5 (20.6–33.4)*	27.3 (21.4–34.3)	26.7 (20.7–33.7)	27.6 (21.7–34.6)	27.1 (21.0–34.0)
Xerostomia	56.1 (50.2–62.9)	53.1 (47.5–58.9)*	56.4 (50.7–63.2)	53.6 (48.1–59.3)*	56.4 (50.6–63.4)	53.6 (48.0–59.4)*

Abbreviations: CI = conformity index; HI = homogeneity index; CMRO = Composite minimax robust optimization; PCM = pharyngeal constrictor muscle; EAGD: estimated actually given dose. The 95% confidence interval values are given between the brackets.

* Statistically significant difference between de PTV-plan and cmRO-plan, using the Wilcoxon signed-rank test adjusted using Bonferroni's correction for multiple testing.

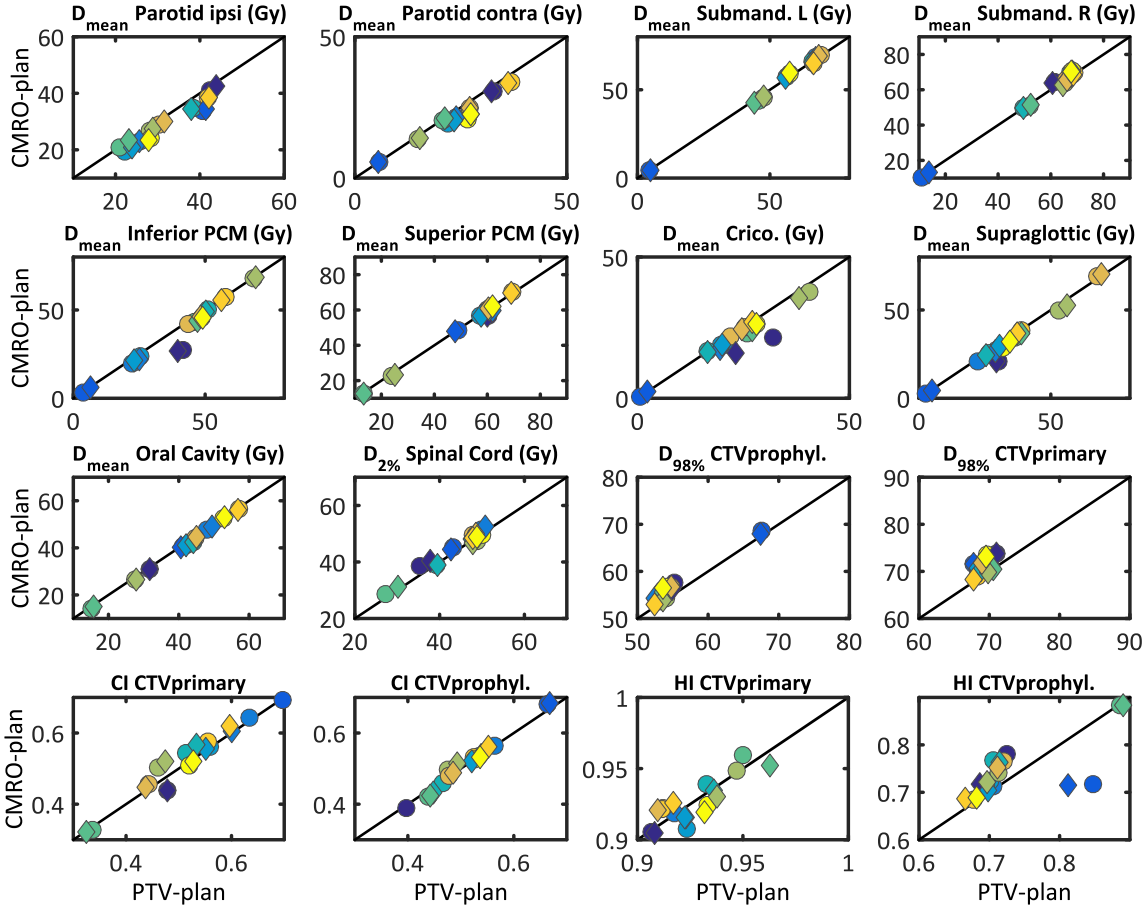

Fig. 3. Estimated actually given dose for PTV optimized and robustly optimized VMAT treatment plans (n = 10). Each scatter plot represents a different dose parameter. The x position of each data point corresponds to its value of the PTV optimized plan and its y position to its value of the robustly optimized plan. Therefore, data points below the diagonal indicate a lower value in the robustly optimized plan than in the PTV optimized plan. Data points shown as circles represent the planned nominal dose and diamond shapes represent the estimated actually given dose.

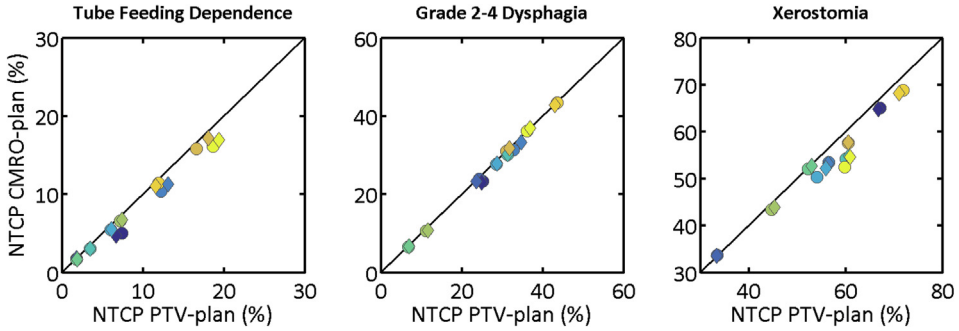

Fig. 4. Estimated normal tissue complication model outcome for PTV optimized and robustly optimized VMAT treatment plans (n = 10). Each scatter plot represents a NTCP model. The x position of each data point corresponds to its value of the PTV optimized plan and its y position to its value of the robustly optimized plan. Therefore, data points below the diagonal indicate a lower value in the robustly optimized plan than in the PTV optimized plan. Data points shown as circles represent the planned nominal dose and diamond shapes represent the estimated actually given dose.

Table 2
The average dosimetric parameters and NTCP values of the non-adaptive and adaptive PTV-based and CMRO-based treatment simulations of four patients.

	EAGD non-adapted plan (N = 4)		EAGD adapted plan (N = 4)	
	PTV-plan	CMRO-plan	PTV-plan	CMRO-plan
Dmean of OARs (Gy)				
Ipsi parotid	27.3 (23.6–29.7)	24.3 (20.0–27.1)	24.3 (20.0–27.1)	24.8 (19.9–28.0)
Contra parotid	25.5 (23.2–27.1)	22.3 (20.3–23.7)	22.3 (20.3–23.7)	21.7 (19.0–23.5)
Submand. Right	62.3 (55.4–67.2)	63.3 (56.5–68.1)	63.3 (56.5–68.1)	62.4 (55.7–67.1)
Submand. Left	67.4 (66.8–68.3)	68.5 (66.8–70.4)	68.5 (66.8–70.4)	67.6 (65.8–69.2)
Inferior PCM	36.4 (21.2–47.1)	34.0 (19.4–44.5)	34.0 (19.4–44.5)	33.0 (18.1–43.5)
Superior PCM	60.4 (57.9–62.2)	60.0 (57.2–61.8)	60.0 (57.2–61.8)	59.3 (57.1–60.8)
Cricopharyngeus M.	23.0 (18.9–25.9)	21.8 (17.8–24.9)	21.8 (17.8–24.9)	21.2 (17.5–23.8)
Supraglottic larynx	40.8 (21.6–53.9)	39.7 (18.8–54.1)	39.7 (18.8–54.1)	38.5 (16.9–53.1)
Oral cavity	47.5 (42.0–51.1)	47.0 (41.0–51.0)	47.0 (41.0–51.0)	46.2 (40.2–50.3)
Spinal cord (D2)	48.9 (47.5–49.8)	49.9 (47.8–51.3)	49.9 (47.8–51.3)	48.9 (46.3–50.5)
Target coverage				
$D_{98\%}$ $CTV_{primary}$ (Gy)	53.7 (52.9–54.5)	55.7 (54.8–56.6)	55.7 (54.8–56.6)	54.3 (51.9–57.2)
$D_{98\%}$ $CTV_{prophylactic}$ (Gy)	69.1 (68.4–69.6)	71.7 (70.6–72.5)	71.7 (70.6–72.5)	71.1 (69.7–72.1)
CI $CTV_{primary}$	0.53 (0.48–0.59)	0.53 (0.48–0.59)	0.53 (0.48–0.59)	0.55 (0.50–0.60)
CI $CTV_{prophylactic}$	0.52 (0.50–0.54)	0.52 (0.50–0.54)	0.52 (0.50–0.54)	0.53 (0.51–0.55)
HI $CTV_{primary}$	0.92 (0.91–0.93)	0.92 (0.92–0.92)	0.92 (0.92–0.92)	0.93 (0.93–0.94)
HI $CTV_{prophylactic}$	0.67 (0.64–0.72)	0.69 (0.64–0.74)	0.69 (0.64–0.74)	0.67 (0.59–0.78)
NTCPs (%)				
Tube feeding dep.	14.1 (7.0–19.1)	12.7 (6.2–17.3)	12.7 (6.2–17.3)	12.2 (5.9–16.5)
Grade 2–4 dysphagia	32.9 (28.8–35.7)	32.5 (28.1–35.4)	32.5 (28.1–35.4)	31.7 (27.6–34.4)
Xerostomia	58.4 (55.6–60.5)	54.4 (51.8–56.2)	54.4 (51.8–56.2)	53.6 (50.1–55.9)

Abbreviations as in Table 1. Only four patients were studied in the adaptive setting. Due to the low sample size, no statistical test was performed.

comparison between dose accumulation using weekly CTs and weekly CBCTs, we estimated that the error introduced by CBCT-based dose mapping and accumulation were comparable. Furthermore, the same plan evaluation procedure was applied to the CMRO-plan and the PTV-plan. Therefore, the impact of the deformable image registration errors on the EAGD of both planning strategies was expected to be negligible. This was further confirmed by the observation that all statistically significant improvements of the CBCT-based EAGD also improved in the CT-based EAGD.

Previous studies compared the robustness of CMRO and PTV-based optimization by shifting the planning CT without dose recalculation, implicitly assuming dose invariance, which could lead to bias in favor of PTV-based optimization [5] or by systematic shifts with a dose recalculation could lead to bias in favor of CMRO [28]. By evaluating the dose on daily CBCTs, the EAGD accounts for geometrical variations and is very close to the actually given dose and not biased toward CMRO or PTV-based optimization. Furthermore, the accuracy of the CBCT-based dose calculation was evaluated against CT-based dose calculations of which the differences were smaller than the benefit of CMRO compared to PTV-based planning.

We did not observe any case with a CTV underdosage, even without plan adaptation. It is likely that the 5.0 mm CTV-PTV margin and a 5.0 mm robustness parameter were overly conservative. Since CMRO led to improved target coverage, fewer plan adaptations are expected. Alternatively, the robustness parameters could be decreased (i.e. <5.0 mm) such that the target coverage equals the coverage of the PTV-plans. This would potentially reduce OAR doses even further. Moreover, the robust objective functions were limited to CTVs only since the distribution of shifts for OAR further away from the treatment isocenter are variable. Taking different shifts for the OARs into account would be too computationally intensive, and will be part of ongoing work.

The main conclusions of the presented work is that target coverage can be improved and OAR dose can be reduced by using CMRO as compared to PTV-based planning in VMAT of HNC patients. Secondly, we conclude that a mid-treatment course plan adaptation further reduces the dose to the OARs by approximately 1 Gy, albeit for a subgroup of patients. Lastly, we found that VMAT plan evaluation on CBCTs leads to similar conclusions with regard to the EAGD compared to weekly repeat CTs. This may potentially

omit the need for repeat CTs for the purpose of plan evaluation if CBCTs are available.

Conflicts of interest

None.

Financial disclosure

Nothing to disclose.

Appendix A. Supplementary data

Supplementary data to this article can be found online at https://doi.org/10.1016/j.radonc.2019.03.019.

References

[1] van Herk M, Remeijer P, Rasch C, Lebesque JV, Van Herk M, Remeijer P, et al. The probability of correct target dosage: dose-population histograms for deriving treatment margins in radiotherapy. Int J Radiat Oncol Biol Phys 2000;47:1121–35.

[2] ICRU. ICRU 50 Prescribing, recording and reporting photon beam therapy. J ICRU 1993.

[3] ICRU. ICRU 83 Prescribing, Recording, and Reporting Photon-Beam Intensity-Modulated Radiation Therapy (IMRT). vol. 10. 2010. doi:10.1093/jicru/ndq025.

[4] Unkelbach J, Bortfeld T, Martin BC, Soukup M. Reducing the sensitivity of IMPT treatment plans to setup errors and range uncertainties via probabilistic treatment planning. Med Phys 2009;36:149–63. https://doi.org/10.1118/1.3021139.

[5] Fontanarosa D, Van Der Laan HP, Witte M, Shakirin G, Roelofs E, Langendijk JA, et al. An in silico comparison between margin-based and probabilistic target-planning approaches in head and neck cancer patients. Radiother Oncol 2013;109:430–6. https://doi.org/10.1016/j.radonc.2013.07.012.

[6] Mahmoudzadeh H, Lee J, Chan TCY, Purdie TG. Robust optimization methods for cardiac sparing in tangential breast IMRT. Med Phys 2015;42:2212–22. https://doi.org/10.1118/1.4916092.

[7] Zhang P, Yorke E, Hu Y-C, Mageras G, Rimner A, Deasy JO. Predictive treatment management: incorporating a predictive tumor response model into robust prospective treatment planning for non-small cell lung cancer. Int J Radiat Oncol Biol Phys 2014;88:446–52. https://doi.org/10.1016/j.ijrobp.2013.10.038.

[8] Bangert M, Hennig P, Oelfke U. Analytical probabilistic modeling for radiation therapy treatment planning. Phys Med Biol 2013;58:5401–19. https://doi.org/10.1088/0031-9155/58/16/5401.

[9] Bohoslavsky R, Witte MG, Janssen TM, van Herk M. Probabilistic objective functions for margin-less IMRT planning. Phys Med Biol 2013;58:3563–80. https://doi.org/10.1088/0031-9155/58/11/3563.

[10] Witte MG, Sonke JJ, Siebers J, Deasy JO, Van Herk M. Beyond the margin recipe: The probability of correct target dosage and tumor control in the presence of a dose limiting structure. Phys Med Biol 2017;62:7874–88. https://doi.org/10.1088/1361-6560/aa87fe.

[11] Birkner M, Yan D, Alber M, Liang J, Nüsslin F. Adapting inverse planning to patient and organ geometrical variation: algorithm and implementation. Med Phys 2003;30:2822–31. https://doi.org/10.1118/1.1610751.

[12] Unkelbach J, Chan TCY, Bortfeld T. Accounting for range uncertainties in the optimization of intensity modulated proton therapy. Phys Med Biol 2007;52:2755–73. https://doi.org/10.1088/0031-9155/52/10/009.

[13] Fredriksson A, Forsgren A, Hårdemark B. Minimax optimization for handling range and setup uncertainties in proton therapy. Med Phys 2011;38:1672–84. https://doi.org/10.1118/1.3556559.

[14] Fredriksson A, Bokrantz R. A critical evaluation of worst case optimization methods for robust intensity-modulated proton therapy planning. Med Phys 2014;41:. https://doi.org/10.1118/1.4883837081701.

[15] van der Laan HP, Christianen M, Bijl HP. The potential benefit of swallowing sparing intensity modulated radiotherapy to reduce swallowing dysfunction: an in silico planning comparative study. Radiother Oncol 2012;103:76–81. https://doi.org/10.1016/j.radonc.2011.11.001.

[16] Harrington D, Schild S, Wong W, Vora S, Liu W. SU-E-T-642: PTV is the voxel-wise worst-case of CTV in prostate photon therapy 3484–3484. Med Phys 2015;42. https://doi.org/10.1118/1.4925005.

[17] Kierkels RGJ, Fredriksson A, Both S, Langendijk JA, Scandurra D, Korevaar EW. Automated robust proton planning using dose-volume histogram-based mimicking of the photon reference dose and reducing organ at risk dose optimization. Int J Radiat Oncol Biol Phys 2018. https://doi.org/10.1016/j.ijrobp.2018.08.023.

[18] Weistrand O, Svensson S. The ANACONDA algorithm for deformable image registration in radiotherapy. Med Phys 2015;42:40–53. https://doi.org/10.1118/1.4894702.

[19] Dice LR. Measures of the amount of ecologic association between species. Ecology 1945;26:297–302. https://doi.org/10.2307/1932409.

[20] Landelijk Platform Protonentherapie. Landelijk Indicatie Protocol Protonen Therapie. 2017. http://www.nvro.nl/publicaties/rapporten.

[21] Wopken K, Bijl HP, van der Schaaf A, van der Laan HP, Chouvalova O, Steenbakkers RJHM, et al. Development of a multivariable normal tissue complication probability (NTCP) model for tube feeding dependence after curative radiotherapy/chemo-radiotherapy in head and neck cancer. Radiother Oncol 2014;113:95–101. https://doi.org/10.1016/j.radonc.2014.09.013.

[22] Bonferroni CE. Statistical theory of classes and probability calculus. Publ R High Inst Econ Commer Sci Florence 1936;8:3–62.

[23] Jensen CA, Roa AMA, Johansen M, Lund J-Å, Frengen J. Robustness of VMAT and 3DCRT plans toward setup errors in radiation therapy of locally advanced left-sided breast cancer with DIBH. Phys Med 2018;45:12–8. https://doi.org/10.1016/j.ejmp.2017.11.019.

[24] Archibald-Heeren BR, Byrne MV, Hu Y, Cai M, Wang Y. Robust optimization of VMAT for lung cancer: dosimetric implications of motion compensation techniques. J Appl Clin Med Phys 2017;18:104–16. https://doi.org/10.1002/acm2.12142.

[25] Zhang P, Hunt M, Happersett L, Yang J, Zelefsky M, Mageras G. Robust plan optimization for electromagnetic transponder guided hypo-fractionated prostate treatment using volumetric modulated arc therapy. Phys Med Biol 2013;58:7803–13. https://doi.org/10.1088/0031-9155/58/21/7803.

[26] Pflugfelder D, Wilkens JJ, Oelfke U. Worst case optimization: a method to account for uncertainties in the optimization of intensity modulated proton therapy. Phys Med Biol 2008;53:1689–700. https://doi.org/10.1088/0031-9155/53/6/013.

[27] Jaffray DA, Lindsay PE, Brock KK, Deasy JO, Tomé WA. Accurate accumulation of dose for improved understanding of radiation effects in normal tissue. Int J Radiat Oncol Biol Phys 2010;76:S135–9. https://doi.org/10.1016/j.ijrobp.2009.06.093.

[28] Miura H, Ozawa S, Nagata Y. Efficacy of robust optimization plan with partial-arc VMAT for photon volumetric-modulated arc therapy: a phantom study. J Appl Clin Med Phys 2017;18:97–103. https://doi.org/10.1002/acm2.12131.